



ELSEVIER

## PHYSICS CONTRIBUTION

# FEASIBILITY OF SYNCHRONIZATION OF REAL-TIME TUMOR-TRACKING RADIOTHERAPY AND INTENSITY-MODULATED RADIOTHERAPY FROM VIEWPOINT OF EXCESSIVE DOSE FROM FLUOROSCOPY

HIROKI SHIRATO, M.D., PH.D., MASATAKA OHTA, R.T., KATSUHISA FUJITA, R.T.,  
YOSHIHARU WATANABE, R.T., AND KAZUO MIYASAKA, M.D., PH.D.

Department of Radiology, Hokkaido University Hospital, Sapporo, Japan

**Purpose:** Synchronization of the techniques in real-time tumor-tracking radiotherapy (RTRT) and intensity-modulated RT (IMRT) is expected to be useful for the treatment of tumors in motion. Our goal was to estimate the feasibility of the synchronization from the viewpoint of excessive dose resulting from the use of fluoroscopy. **Methods and Materials:** Using an ionization chamber for diagnostic X-rays, we measured the air kerma rate, surface dose with backscatter, and dose distribution in depth in a solid phantom from a fluoroscopic RTRT system. A nominal 50–120 kilovoltage peak (kVp) of X-ray energy and a nominal 1–4 ms of pulse width were used in the measurements.

**Results:** The mean  $\pm$  SD air kerma rate from one fluoroscope was  $238.8 \pm 0.54$  mGy/h for a nominal pulse width of 2.0 ms and nominal 100 kVp of X-ray energy at the isocenter of the linear accelerator. The air kerma rate increased steeply with the increase in the X-ray beam energy. The surface dose was 28–980 mGy/h. The absorbed dose at a 5.0-cm depth in the phantom was 37–58% of the peak dose. The estimated skin surface dose from one fluoroscope in RTRT was 29–1182 mGy/h and was strongly dependent on the kilovoltage peak and pulse width of the fluoroscope and slightly dependent on the distance between the skin and isocenter.

**Conclusion:** The skin surface dose and absorbed depth dose resulting from fluoroscopy during RTRT can be significant if RTRT is synchronized with IMRT using a multileaf collimator. Precise estimation of the absorbed dose from fluoroscopy during RT and approaches to reduce the amount of exposure are mandatory.  
© 2004 Elsevier Inc.

Real-time tumor-tracking radiotherapy, Fluoroscopy, Dosimetry.

## INTRODUCTION

Fluoroscopic detection of internal fiducial markers for precise setup of patients has been shown to be useful for static radiotherapy (RT) (1–5) and real-time tracking and gated RT (6–10). Prototype real-time tumor-tracking RT (RTRT) uses two sets of fluoroscopy to detect the internal motion of a metallic fiducial marker in or near the target volume (1). Attention to four-dimensional accuracy in space and time is increasing for tumors in motion when the meticulous dose distribution used in particle therapy (11) and intensity-modulated RT (IMRT) (12–17). Synchronization of IMRT and RTRT is expected to increase the therapeutic ratio for tracking moving tumors.

In our previous studies of RTRT without IMRT, the dose rate in the phantom was measured with thermoluminescence and a surface dosimeter (12, 16). The dose rate at 120 kV with a pulse width of 4 ms was 10.8 mGy/min at the entrance. We concluded that the fluoroscopic dose is negligible for patients treated with 60 Gy to the isocenter.

However, because the beam-on time will be longer when we combine RTRT with IMRT using a multileaf collimator, integration of IMRT and RTRT could result in an extremely long treatment time. IMRT using a multileaf collimator requires a radiation time four to five times longer than conventional RT. This may result in unacceptable exposure from the fluoroscopy.

Interventional neuroradiology requires fluoroscopic examination for >30 min, on average, and is known to result in a noticeably high skin dose (18). Gkanatsios *et al.* (19) have shown that the median surface dose during a neuroradiologic diagnostic imaging examination is 1.3 Gy, with a maximal surface dose as great as 5.1 Gy.

These results suggest the importance of precise dose measurement in RTRT when the treatment time needs to be longer than previously estimated. We measured the dose resulting from the use of fluoroscopy in the RTRT system.

Reprint requests to: Hiroki Shirato, M.D., Ph.D., Department of Radiology, Hokkaido University School of Medicine, North-15 West-7, Kita-ku, Sapporo 006-8638, Japan. Tel: (+81)11-706-5975; Fax (+81) 11-706-7876; E-mail: hshirato@radi.med.hokudai.ac.jp

Partly supported by a grant-in-aid from the Japanese Ministry of Education, Sports, Culture, and Science.

Received Oct 21, 2003, and in revised form Apr 2, 2004.  
Accepted for publication Apr 5, 2004.

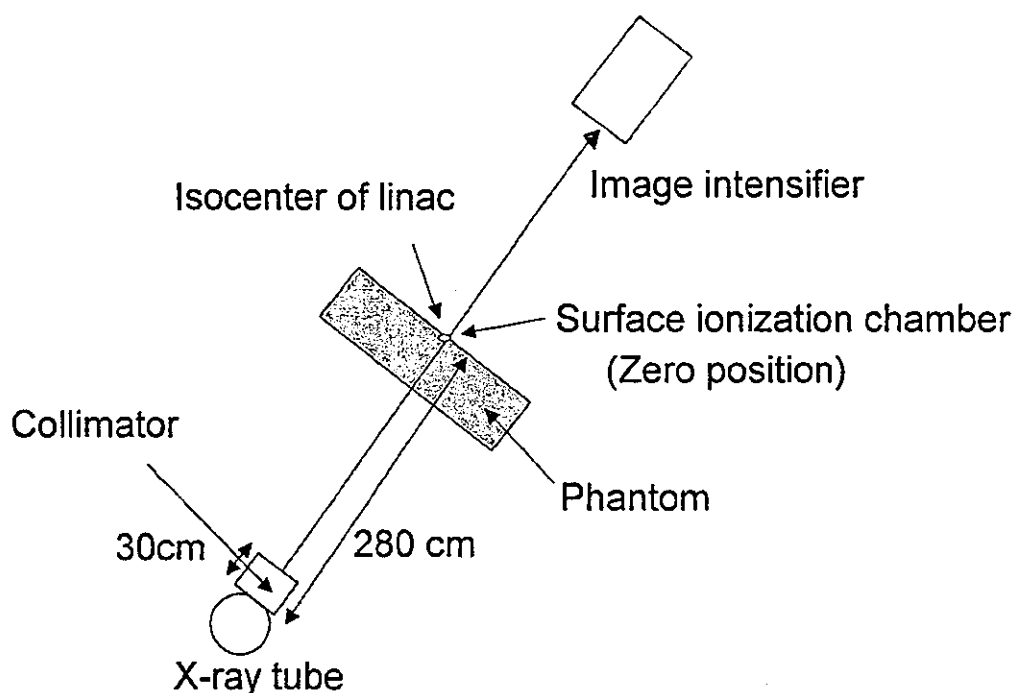


Fig. 1. Geometry of experiments used in this study. Linac = linear accelerator.

## METHODS AND MATERIALS

### Fluoroscopy

The fluoroscope was a rotating anode X-ray tube assembly (G-1582 BI, Shimadzu, Kyoto, Japan) powered by a three-phase generator. Photons were produced by a  $0.6 \times 0.6$  mm<sup>2</sup> nominal size electron beam incident on a rotating target. We used a pulsed cathode of 80 mA, because it is commonly used clinically. For peak tube potentials of 50–120 kilovoltage peak (kVp), the pulse rate used was a nominal 30 s, with pulse duration of 1.2, 1.6, 2.0, 2.5, and 3.2 ms. The power of the X-ray tube was 1500 kJ for a 0.6-mm focus and 1060 kJ for a 1.0-mm focus. The inherent X-ray filtration was 1.5 mm aluminum equivalent.

The geometries of the fluoroscopy and measurement are shown in Fig. 1. The X-ray beam was collimated to visualize the image of the fiducial markers, which should be placed close to the isocenter. The distance from the X-ray tube to the image detector was 460 cm to avoid collision between the image detectors and the gantry of the linear accelerator. The distance from the X-ray tube (target) to the isocenter of the linear accelerator was 280 cm. The fluoroscopic beam was collimated to  $1.6 \times 1.9$  cm at a 30-cm distance from the tube. The beam size enlarged to  $14.5 \times 18.5$  cm<sup>2</sup> at the isocenter of the linear accelerator where the measurement was performed.

### Measurement

The fluoroscopy irradiated field was measured in air using film at the plane including the isocenter perpendicular to the beam axis of the diagnostic X-ray.

The air kerma was measured with a cylindrical chamber

with a collecting volume of 3 cm<sup>3</sup>, using a Scanditronix WELLHOFER DC300 TNC/160 and a RAMTEC 1500B (Toyo Medic, Tokyo, Japan) designed for diagnostic radiography and mammography. The nominal X-ray energy available for measurement was quoted as 20–150 kV. The wall of the chamber was made of Shonka C552 (1.7 g/cm<sup>3</sup>) with the thickness at 0.3 mm. The chamber has an outer length of 41.5 mm and an outer diameter of 10.6 mm. The nominal calibration factor was 9.3 mGy/nC.

The half value layer was measured using varying thicknesses (0.25, 1.05, and 2.05 mm) of a 20.0 × 30.0-cm aluminum (Al) sheet (99.999% Al). The half value layer was measured using a source-to-aluminum filtration distance of 25 cm and a source-to-detector distance of 280 cm.

The dose in air at the isocenter was measured to estimate the air kerma, which does not take into account any backscatter. The distance from the X-ray source to the central axis of the chamber was 280 cm, and the field size was  $10 \times 14$  cm<sup>2</sup>. The chamber was positioned on the central axis of the beam, with its long axes parallel to the cathode–anode direction of the X-ray tube.

The percent depth dose (PDD) was measured with a smaller chamber, a farmer-type chamber No. 2591 with a collecting volume of 0.6 cm<sup>3</sup> without a build-up cap in the Solid Water phantom. The ionization chamber was placed on the surface of the phantom, which consisted of  $30 \times 30$ -cm<sup>2</sup> slabs of Solid Water, with a total thickness of 10 cm (Fig. 1). The source-to-surface distance was set at 280 cm from the tube. The dose rate at 0.0, 1.0, 2.0, 3.0, 4.0, 5.0, 6.0, 8.0, 10, 12, 15, and 20 cm was measured by changing the depth of the chamber perpendicular to the beam axis for

Table 1. Measured air kerma rate from one fluoroscope at isocenter of linear accelerator according to nominal kVp

Air kerma rate	Nominal kVp			
	50	70	100	120
Mean (mGy/h)	33.50	90.25	238.80	366.18
SD (mGy/h)	0.30	0.15	0.54	0.86
%SD	0.9	0.2	0.2	0.2

Abbreviation: kVp = kilovoltage peak.

a nominal 50-, 70-, 100-, and 120-kVp X-ray beam, respectively. The depth of the chamber was adjusted by adding the corresponding  $30 \times 30$ -cm<sup>2</sup> slabs of Solid Water, with a total thickness of 1.0–20 cm on the surface of the phantom. The position of the chamber was adjusted to be on the central X-ray beam axis and parallel to the cathode–anode direction of the X-ray tube by visualizing the chamber under fluoroscopy. Correction was made for recombination, polarity, or energy dependence effects. The “surface” measurement at depth 0 was acquired with the center of the cylindrical chamber put at the same plane as the surface of the Solid Water phantom by cutting the surface of the phantom to fit it in. The PDD was normalized at the depth of the maximal dose for each X-ray beam.

The mean  $\pm$  standard deviation were calculated for each data item on the basis of 10 measurements for each data point.

## RESULTS

The half-value layer for each nominal kilovoltage peak of the X-ray tube was estimated to be 2.73, 3.71, 5.02, and 6.72

mm Al for a nominal 50, 70, 100, and 120-kVp X-ray beam, respectively.

The air kerma rate from one fluoroscope was  $20.3 \pm 0.2$ ,  $26.3 \pm 0.4$ ,  $33.5 \pm 0.3$ ,  $47.9 \pm 0.2$ , and  $68.2 \pm 0.3$  mGy/h at a nominal pulse width of 1.2, 1.6, 2.0, 2.8, and 4.0 ms, respectively, with a nominal 50-kVp X-ray beam. The air kerma rate from simultaneous exposure of two fluoroscopes with a nominal 50-kVp X-ray beam for 1.6 and 2.0 ms was  $58.7 \pm 0.5$  and  $72.7 \pm 0.3$  Gy/h respectively, which was roughly twice (2.2 times the rate with one fluoroscope) the corresponding dose rate of one fluoroscope.

The air kerma rate measured for one X-ray tube at the isocenter of the linear accelerator is shown in Table 1 for each nominal kilovoltage peak of the X-ray tube using 2.0 ms as the pulse width. The air kerma rate from one fluoroscope was  $238.8 \pm 0.54$  mGy/h for a nominal pulse width of 2.0 ms with a nominal 100-kVp X-ray beam. The relationship between the nominal kilovoltage peak and the air kerma rate is shown in Fig. 2. The air kerma rate increased steeply with the increase in the X-ray beam energy.

The relationship between the pulse width and the surface dose rate, including backscatter, is shown in Fig. 3 according to the nominal kilovoltage peak. The surface dose was 28–980 mGy/h (Table 2). The surface dose was strongly dependent on the kilovoltage peak and linearly increased with the pulse width of the fluoroscope.

The PDD curves for each nominal kilovoltage peak of the X-ray beam are shown in Fig. 4. The dose at 5.0 cm was 37–58% for 50–120 kVp, respectively.

When we put a patient on the treatment couch, the patient's skin surface will receive a greater dose than the dose estimated at the isocenter because of the shorter distance from the X-ray source to the skin surface. Assuming that the distance between the skin entrance and the isocenter,  $r$ , is

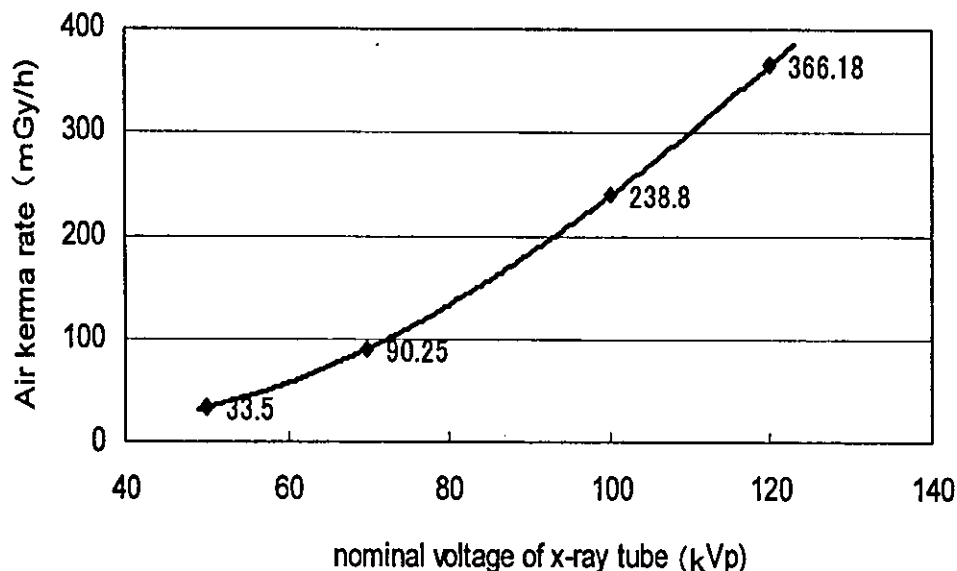


Fig. 2. Relationship between nominal kilovoltage peak of fluoroscopic X-ray and air kerma rate from one fluoroscope.

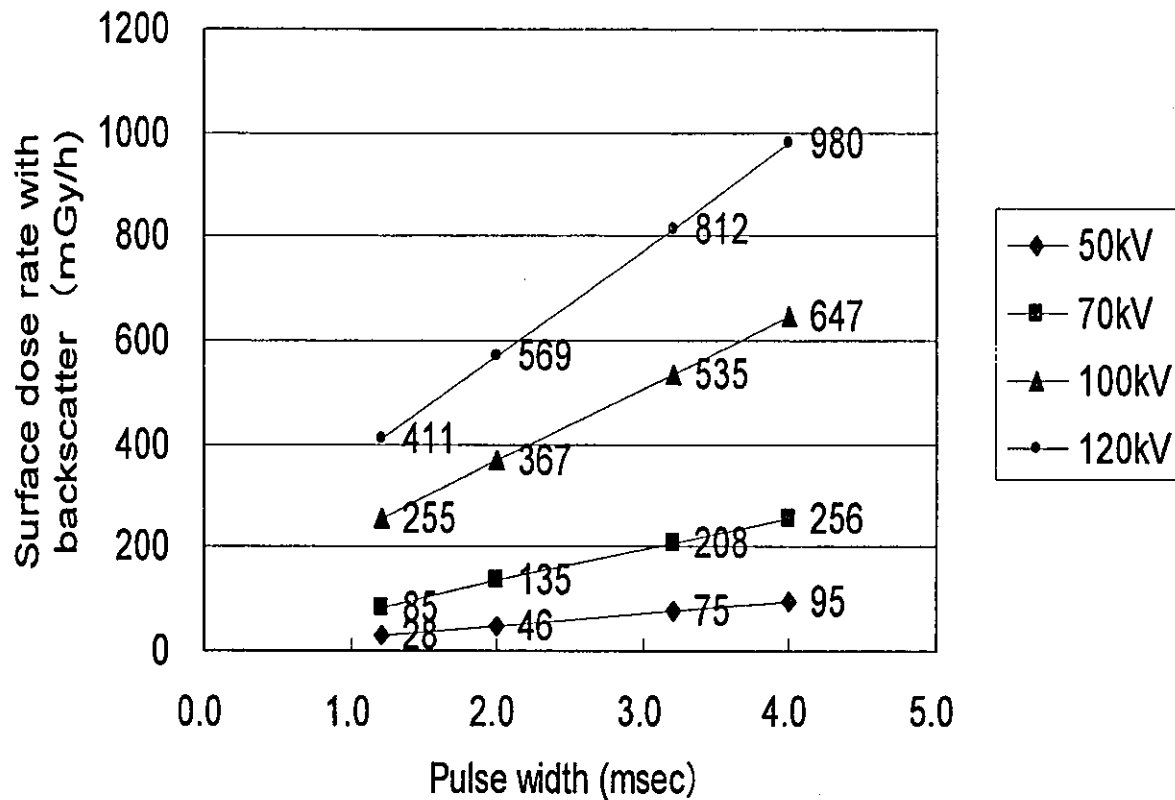


Fig. 3. Relationship between pulse width and surface dose rate from one fluoroscope according to kilovoltage peak. Diamonds, 50 kV; squares; 70 kV, triangles; 100 kV; circles, 120 kV.

5–25 cm, the estimated dose at the skin surface with backscatter (Fig. 5) will be from  $r = 5$  cm to  $r = 25$  cm. The dose was calculated simply using the formula  $R^2/(Rr)^2$ , where  $R$  is the distance from the X-ray source to the isocenter (280 cm in the RTRT system). The estimated skin surface dose from one fluoroscope in RTRT was 29–1182 mGy/h. The estimated skin surface dose was strongly dependent on the kilovoltage peak and the pulse width of the fluoroscope and slightly dependent on the distance between the skin and isocenter.

## DISCUSSION

The Joint Working Party of the British Institute of Radiology and the Hospital Physicists' Association published

Table 2. Estimated dose rate at skin surface for different pulse widths and kVp values

Pulse width (ms)	Estimated dose rate (mGy/h)			
	50 kVp	70 kVp	100 kVp	120 kVp
1.2	28.4	483.2	255.2	411
2.0	45.9	762.2	366.8	568.5
3.2	75.4	1174.4	535	811.7
4.0	94.7	1448.7	647.4	980.1

Abbreviation: kVp = kilovoltage peak.

PDD curves of similar beams measured for use in RT (20). Jennings and Harrison (21) and Harrison (22) have also published the depth dose of diagnostic radiography. Fetterly *et al.* (23) published the X-ray dose distribution of fluoroscopy beams in 2001. These data were based on the measurements using source-to-surface distances of 30–50 cm, far shorter than the source-to-surface distance of 280 cm used in the RTRT system. The greater percentage of dose at each depth in our study compared with those in previous reports for kilovoltage of X-rays may be a result of the longer source-to-surface distance in the RTRT system. We were not able to measure the “surface dose” by parallel chamber with sufficient sensitivity and used a 0.6-cm<sup>3</sup> cylindrical chamber, which could also have been a source of bias in our study. More work is required for precise measurement.

The real-time tumor-tracking system has been used with precise setup and gated RT in >200 patients with various tumors, including head-and-neck tumors and tumors of the lung, esophagus, liver, pancreas, prostate, and uterus (1). In this study, we investigated the parameters used in actual RTRT for various tumors. A nominal X-ray strength of 80 kVp and pulse width of 2–4 ms are frequently used for the head-and-neck region, and a strength of 100–120 kVp and duration of 2 ms are used for lung and liver treatment in clinical practice. If the patient's body is large or thick, the system requires 4 ms for visualization of the internal marker.

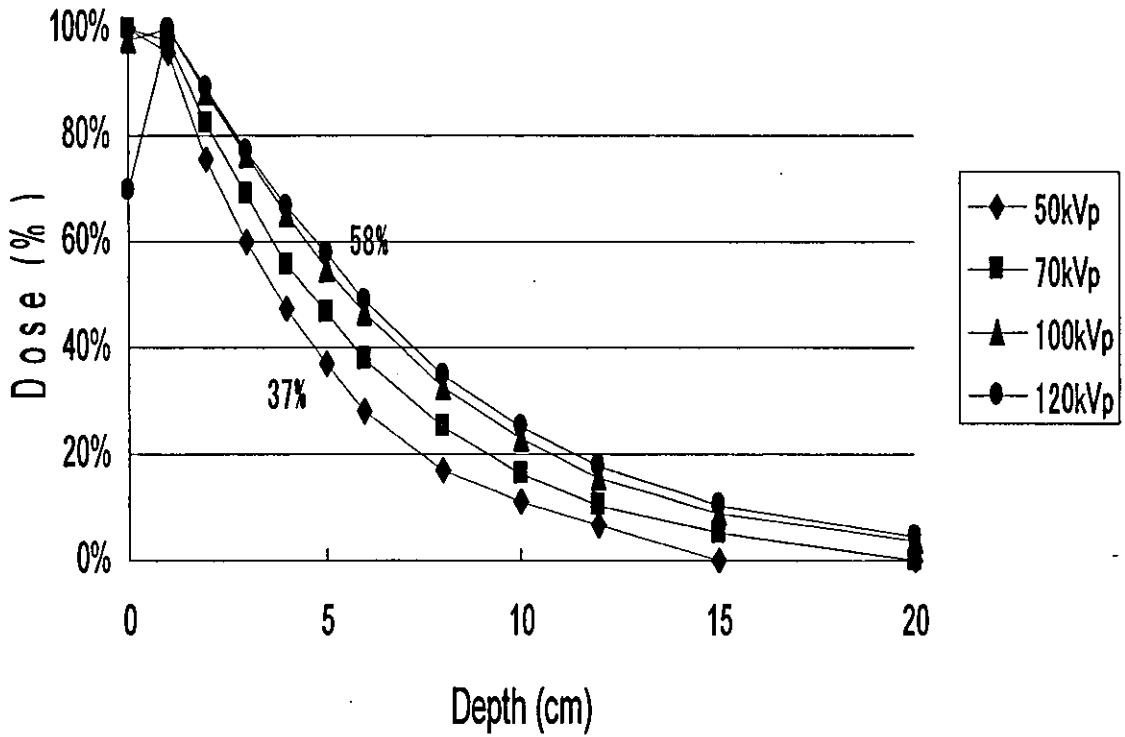


Fig. 4. Percent depth dose curves according to kilovoltage peak of fluoroscope. Diamonds, 50 kV; squares; 70 kV, triangles; 100 kV; circles, 120 kV.

Because RTRT usually requires two sets of fluoroscopy, the maximal dose possible to deliver to the skin surface is two times the dose at the skin surface from one fluoroscope. Usually, the two diagnostic beams do not overlap at the skin surface. However, they could overlap if treating a tumor

very close to the skin surface. With the expected RT times needed for IMRT plus RTRT and the exposure parameters required for sufficient image quality, the patient exposure could be unacceptable.

A normal (four fields), 2-Gy, static field treatment is

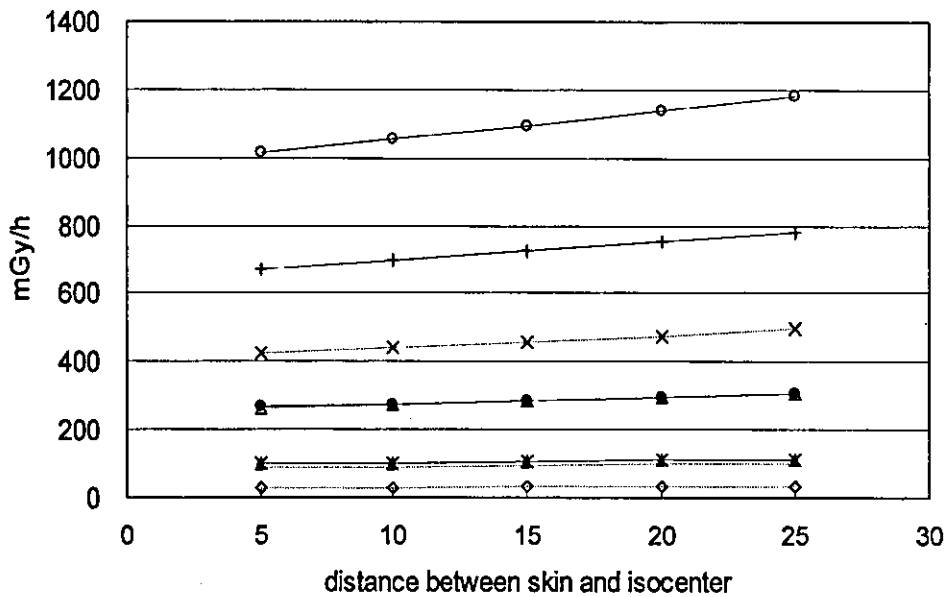


Fig. 5. Relationship between distance from surface to isocenter and surface dose rate from one fluoroscope. Diamonds, 50 kVp, 1.2 ms; asterisks, 50 kVp, 4.0 ms; squares, 70 kVp, 1.2 ms; black circles, 70 kVp, 1.4 ms; triangles, 100 kVp, 1.2 ms; plus signs, 100 kVp, 1.4 ms; crosses, 120 kVp, 1.2 ms; white circles, 120 kVp, 1.4 ms.

≤300 MU approximately. At 300 MU/min and a 25% duty cycle, this would equal 4 min of surveillance time or a skin dose of ~8 cGy (highest case, 120 kVP and 4 ms [Fig. 5], 4 min/60 min × 1.2 Gy/h). If IMRT increases the monitor unit (MU) by a factor of 3–5, the treatment time should be only 12–20 min; however, the fluoroscopic dose becomes worrisome, not so much at the skin but at depth, for which the PDD may not be insignificant. In practice, we have noted that intrafractional fluctuation of tumor motion is often so large that the table position must be adjusted several times by additional fluoroscopic examination (8). In that case, the fluoroscopic dose could extend to 30 min.

In interventional neuroradiology, advances in insertion techniques and catheter materials have increased the acceptable exposure time of diagnostic radiography. The unexpectedly high doses used in modern interventional radiology have raised concerns about radiation safety and protection (18). The results of the present study have confirmed that it is also important to reduce the radiation dose from fluoroscopic exposure during RT. A reduction of the field size is important, but not the perfect answer, because the same area of skin will receive the same dose every day during RTRT. Sharp *et al.* (24) have found that various prediction models, such as a linear model or neural network model, can help reduce the pulse rate to <30 Hz. They considered 14 lung tumor cases in which the peak-to-peak motion was >8 mm and compared the localization error using linear prediction, neural network prediction, and Kalman filtering against a system that used no prediction. They found that by using prediction, the root mean squared error between the predicted and actual three-dimensional (3D) motion was improved for all latencies and all imaging rates evaluated. A reduction in the source-to-detector distance is also useful to reduce the amount of exposure. The attachment of the X-ray tubes and cameras to the gantry head of the linear accelerator can reduce the source-to-detector distance significantly (17). The amount of reduction in the absorbed dose will be about one-third of that of our system, providing that the same dose is required at the surface of the image intensifier. Amorphous silicon detectors may reduce the dose required to obtain an image with the same time resolution; the

absorbed dose will be further reduced. Changing the fluoroscopy angle according to changes in the therapeutic beam angle beam may also help to reduce the dose to the same skin surface. The shortcoming of the gantry-mounted imaging units may be their inability to use noncoplanar irradiation techniques and the difficulty in maintaining imaging unit accuracy. Also, the X-ray tubes and image detectors can be an obstacle during non-RTRT. Magnetic detection of the metallic marker in the body can eliminate the requirement for fluoroscopic exposure and is also expected to be an alternative to the fluoroscopic detection of internal fiducial markers (25).

We have adapted several approaches to reduce the amount of exposure from fluoroscopy to synchronize RTRT and IMRT. First, software was designed that allows the use of one instead of two sets of fluoroscopy for tracking after registration between the 3D coordinates and the two-dimensional projected coordinates of the marker on one fluoroscopic image. The shortcoming of this method is that two-dimensional projection does not provide information about the third dimension; thus, we have not yet used the two-dimensional projection method in a clinical situation. Second, the pulse rate is now changeable from 30 Hz to 15, 10, 5, and 2 Hz. If the tumor is moving slowly, the lower pulse rate can be used. Third, a 3D trajectory of the tumor is obtained before actual treatment and is used to select the best position for tracking each day to improve gating efficiency. We plan to include the 3D dose distribution of the fluoroscopic beam in our treatment planning system to combine it with the dose distribution of the therapeutic beams. Details of these developments will be described elsewhere.

## CONCLUSION

The absolute dose and depth-dose distribution of fluoroscopy in the RTRT system showed that synchronization of RTRT and IMRT may result in an unacceptably high radiation dose to the skin surface and possibly to the deep tissues. The synchronization of RTRT and IMRT requires improvement to reduce fluoroscopic exposure.

## REFERENCES

1. Shirato H, Harada T, Harabayashi T, *et al.* Feasibility of insertion/implantation of 2.0-mm-diameter gold internal fiducial markers for precise setup and real-time tumor tracking in radiotherapy. *Int J Radiat Oncol Biol Phys* 2003;56:240–247.
2. Shimizu S, Shirato H, Kitamura K, *et al.* Use of an implanted marker and real-time tracking of the marker for the positioning of prostate and bladder cancers. *Int J Radiat Oncol Biol Phys* 2000;48:1591–1597.
3. Kitamura K, Shirato H, Shimizu S, *et al.* Registration accuracy and possible migration of internal fiducial gold marker implanted in prostate and liver treated with real-time tumor-tracking radiation therapy (RTRT). *Radiother Oncol* 2002;62:275–281.
4. Kaatee RS, Olofsen MJ, Verstraate MB, *et al.* Detection of organ movement in cervix cancer patients using a fluoroscopic electronic portal imaging device and radiopaque markers. *Int J Radiat Oncol Biol Phys* 2002;54:576–583.
5. Poggi MM, Gant DA, Sewchand W, *et al.* Marker seed migration in prostate localization. *Int J Radiat Oncol Biol Phys* 2003;56:1248–1251.
6. Shimizu S, Shirato H, Ogura S, *et al.* Detection of lung tumor movement in real-time tumor-tracking radiotherapy. *Int J Radiat Oncol Biol Phys* 2001;51:304–310.
7. Kubo HD, Wang L. Introduction of audio gating to further reduce organ motion in breathing synchronized radiotherapy. *Med Phys* 2002;29:345–350.
8. Seppenwoolde Y, Shirato H, Kitamura K, *et al.* Precise and real-time measurement of 3D tumor motion in lung due to breathing and heartbeat, measured during radiotherapy. *Int J Radiat Oncol Biol Phys* 2002;53:822–834.

9. Harada T, Shirato H, Ogura S, *et al.* Real-time tumor-tracking radiation therapy for lung carcinoma by the aid of insertion of a gold marker using bronchofiberscopy. *Cancer* 2002;95:1720-1727.
10. Kitamura K, Shirato H, Seppenwoolde Y, *et al.* Tumor location, cirrhosis, and surgical history contribute to tumor movement in the liver, as measured during stereotactic irradiation using a real-time tumor-tracking radiotherapy system. *Int J Radiat Oncol Biol Phys* 2003;56:221-228.
11. Minohara S, Kanai T, Endo M, *et al.* Respiratory gated irradiation system for heavy-ion radiotherapy. *Int J Radiat Oncol Biol Phys* 2000;47:1097-1103.
12. Shirato H, Shimizu S, Kitamura K, *et al.* Four-dimensional treatment planning and fluoroscopic real-time tumor tracking radiotherapy for moving tumor. *Int J Radiat Oncol Biol Phys* 2000;48:435-442.
13. Vedam SS, Keall PJ, Kini VR, *et al.* Acquiring a four-dimensional computed tomography dataset using an external respiratory signal. *Phys Med Biol* 2003;48:45-62.
14. Ford EC, Mageras GS, Yorke E, *et al.* Respiration-correlated spiral CT: A method of measuring respiratory-induced anatomic motion for radiation treatment planning. *Med Phys* 2003;30:88-97.
15. Brock KK, Hollister SJ, Dawson LA, *et al.* Technical note: Creating a four-dimensional model of the liver using finite element analysis. *Med Phys* 2002;29:1403-1405.
16. Shirato H, Shimizu S, Kunieda T, *et al.* Physical aspects of a real-time tumor-tracking system for gated radiotherapy. *Int J Radiat Oncol Biol Phys* 2000;48:1187-1195.
17. Neicu T, Shirato H, Seppenwoolde Y, *et al.* Synchronized moving aperture radiation therapy (SMART): Average tumour trajectory for lung patients. *Phys Med Biol* 2003;48:587-598.
18. Kemerink GJ, Frantzen MJ, Oei K, *et al.* Patient and occupational dose in neurointerventional procedures. *Neuroradiology* 2002;44:522-528.
19. Gkanatsios NA, Huda W, Peters KR. Adult patient doses in interventional neuroradiology. *Med Phys* 2002;29:717-723.
20. Joint Working Party of the British Institute of Radiology and the Hospital Physicists' Association. Central axis depth dose data for use in radiotherapy. *Br J Radiol* 1996;(Suppl. 25).
21. Jennings WA, Harrison RM. X-rays: Half-value thickness range 0.01-8.0 mm Al. *Br J Radiol* 1983;17:1-7.
22. Harrison RM. Central-axis depth-dose data for diagnostic radiology. *Phys Med Biol* 1981;26:657-670.
23. Fetterly KA, Gerbi BJ, Alaci P, *et al.* Measurement of the dose deposition characteristics of x-ray fluoroscopy beams in water. *Med Phys* 2001;28:205-209.
24. Sharp G, Jiang SB, Shimizu S, *et al.* Prediction of respiratory tumor motion for real-time image-guided radiotherapy. *Phys Med Biol* 2004;49:425-440.
25. Seiler PG, Blattmann H, Kirsch S, *et al.* A novel tracking technique for the continuous precise measurement of tumour positions in conformal radiotherapy. *Phys Med Biol* 2000;45: N103-N110.

Technical note

## High dose three-dimensional conformal boost (3DCB) using an orthogonal diagnostic X-ray set-up for patients with gynecological malignancy: a new application of real-time tumor-tracking system

Ritsu Yamamoto<sup>a</sup>, Akio Yonesaka<sup>b</sup>, Seiko Nishioka<sup>b</sup>, Hidemichi Watari<sup>a</sup>,  
Takayuki Hashimoto<sup>b</sup>, Daichi Uchida<sup>b</sup>, Hiroshi Taguchi<sup>a</sup>, Takeshi Nishioka<sup>b</sup>,  
Kazuo Miyasaka<sup>b</sup>, Noriaki Sakuragi<sup>a</sup>, Hiroki Shirato<sup>b,\*</sup>

<sup>a</sup>*Gynecology, Reproductive and Developmental Medicine, Division of Pathophysiological Science, Hokkaido University Graduate School of Medicine, Kita 15, Nishi 7, Kita-Ku, Sapporo 060-8638, Japan*

<sup>b</sup>*Department of Radiology, Hokkaido University Hospital, Sapporo, Japan*

Received 28 November 2003; received in revised form 23 June 2004; accepted 9 August 2004

Available online 30 September 2004

### Abstract

The feasibility and accuracy of high dose three-dimensional conformal boost (3DCB) using three internal fiducial markers and a two-orthogonal X-ray set-up of the real-time tumor-tracking system on patients with gynecological malignancy were investigated in 10 patients. The standard deviation of the distribution of systematic deviations ( $\Sigma$ ) was reduced from 3.8, 4.6, and 4.9 mm in the manual set-up to 2.3, 2.3 and 2.7 mm in the set-up using the internal markers. The average standard deviation of the distribution of random deviations ( $\sigma$ ) was reduced from 3.7, 5.0, and 4.5 mm in the manual set-up to 3.3, 3.0, and 4.2 mm in the marker set-up. The appropriate PTV margin was estimated to be 10.2, 12.8, and 12.9 mm in the manual set-up and 6.9, 6.7, and 8.3 mm in the gold marker set-up, respectively, using the formula  $2\Sigma + 0.7\sigma$ . Set-up of the patients with three markers and two fluoroscopy is useful to reduce PTV margin and perform 3DCB.

© 2004 Published by Elsevier Ireland Ltd.

**Keywords:** Image-guided radiotherapy; Set-up error; Real-time tracking system; Intra-fractional error; Uterine cervix; Vagina; Carcinoma

### 1. Introduction

Uterine cervical cancers are curable with radiotherapy with or without chemotherapy in cases in which a sufficient dose can be given to the clinical target volume (CTV), which includes the gross tumor volume (GTV) and surrounding sub-clinical or microscopic tumor extension [2,5,8]. However, it is sometimes quite difficult, even when the operator is highly skilled, to produce a sufficient dose distribution in patients with a narrow vagina or with relapses at the cervical stump by intracavitary radiotherapy (ICR) [3]. A small but definite number of patients are not treatable with standard radiotherapy due to the inability to insert the tandem into the cervical os. Interstitial radiotherapy is often

helpful in such cases, but its success rate is strongly dependent on the skill of the operator.

It is anticipated that external radiotherapy will be an alternative to ICR or interstitial radiotherapy for patients who cannot be treated with standard radiotherapy. However, a fundamental shortcoming of external radiotherapy is that detrimental set-up error and internal organ motion may occur. To overcome the shortcoming of external radiotherapy, we have developed a fluoroscopic real-time tumor tracking radiotherapy (RTRT) system [11]. We have previously reported the usefulness of orthogonal X-ray imaging by the RTRT system as a precise set-up procedure for prostate cancer [6,7,10,12]. The purpose of the present study was to investigate the feasibility of set-up using three internal fiducial markers and fluoroscopic measurements for gynecological malignancy. Additionally, uncertainties in usual manual set-up were calculated using the accumulated

\* Corresponding author.



data in the RTRT system. Appropriate margins for planning target volume were estimated using the population-based methods both in manual set-up and in the set-up using RTRT system.

## 2. Materials and methods

The real-time tumor-tracking system consisted of two or four sets of fluoroscopes equipped with a conventional linear accelerator in a radiotherapy room (Mitsubishi Electronics Co., Ltd, Tokyo), as reported in a previous study [11]. In brief, the fluoroscopes were equipped obliquely to the position of the table to reduce the thickness of the human body passed by the diagnostic X-ray and to improve the visibility of the fiducial markers. Using two sets of fluoroscopic images, it has previously been shown that the 3D coordinates of the three markers can be determined with an accuracy of  $\pm 0.5$  mm in static phantoms [11].

If ICR and interstitial radiotherapy were abandoned and the patients agreed to enter this study, three 2 mm-radiopaque gold markers (99.9% Au) were implanted in or near the tumor by a trans-vaginal approach using specially-made equipment (Medikit Co., Ltd, Tokyo). After gold markers were implanted, a CT-scan was performed using 1 mm slice thickness for the level involving the tumor mass and three markers. The coordinates of the CTV and three markers were registered and sent to the website of the RTRT system online.

Assuming that the tumor is solid and the 3D relationship between the tumor and the marker does not change significantly, the tumor position can be adjusted to the planned position by translational parallel shift of the treatment couch. After performing the manual set-up of patients on the treatment couch using skin markers and laser localizers in the treatment room by the usual method, two orthogonal fluoroscopic images were taken using the RTRT system. The 3D distance between each marker was calculated using a software in the RTRT system. If the deviation of the 3D distance between each marker was larger than 3.0 mm comparing to the planning CT at the initial treatment day, we assumed that gold marker had migrated from the initial position during the period between CT scan and treatment and thus the fiducial markers were not used for further set-up. If there was less deviation, we assumed that there was no significant migration of the marker and commenced set-up using the three markers. The difference between the coordinates of the center of gravity of the three markers from the planned position relative to the isocenter was calculated and adjusted by moving the treatment couch [7]. After this adjustment, the irradiation was delivered. During the irradiation, fluoroscopic images can be taken at a speed of 2–30 times a second, and one of the markers can be tracked automatically by a real-time pattern recognition algorithm. However, real-time tracking of the marker during the irradiation was not routinely

performed for gynecologic malignancy because it was assumed that minimal intra-fractional movement of the target volume would occur in this protocol setting [8]. We took two orthogonal X-ray images while the gantry was moving to the next portal angle and calculated the intra-fractional shift of the center of gravity of the three markers several times during each treatment. If the shift was larger than 3–5 mm, the table position was corrected and the treatment was continued. No external immobilization device was used throughout the planning and treatment.

We call this boost technique as three-dimensional conformal boost (3DCB) in this study. The multi-leaf collimator consisted of 60 leaves of 5 mm width at the isocenter inside of  $10 \times 10$  cm<sup>2</sup> field and 10 mm width outside of the field, respectively.

As an example of the data analysis, Fig. 1 shows the pooled data of the discrepancy between the planned and actual coordinates of the center of gravity in one patient over four treatment days plotted against the minutes after the manual set-up on the treatment couch. At time zero, the patient is positioned using laser beam localizers to the skin surface so that the discrepancy at time zero is attributed to the set-up error after manual set-up. The couch is adjusted between time 0 and 2 min using gold marker. At 2 min, the position of the marker gradually changed, suggesting intra-fractional organ motion or involuntary movement of the patient. The table position was adjusted again before the start of the next portal irradiation. From 2 to 17 min, the discrepancy was distributed from  $-2.47$  to 3.65 mm and required adjustment of the table position during irradiation several times each day for this patient.

In this study, the inter-fractional set-up error (i.e., external error) both in the manual set-up and in the internal gold marker set-up, and the intra-fractional internal organ motion (i.e., internal error) were analyzed from the coordinates of the center of gravity of three internal gold markers which were stored automatically in the RTRT system in each set-up. Since two orthogonal X-ray images were taken within a period of several minutes, the organ

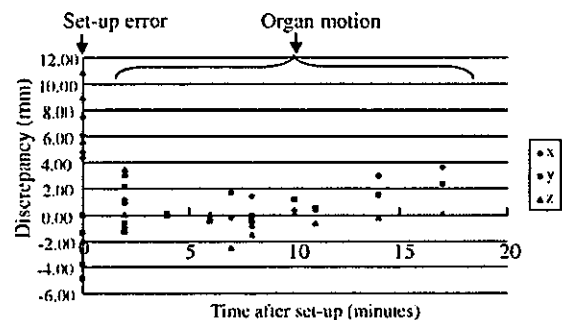


Fig. 1. Discrepancy in mm between the planned and actual positions of the center of gravity of three internal fiducial markers according to the time after manual set-up (time zero) followed by set-up and verification using orthogonal X-ray images. The discrepancy over 2–17 min is consistent with error due to organ motion and patient motion. The data points in four sessions of irradiation were overlapped in this figure.

motion or patient motion over this period can be detected. The rotation angle of the actual coordinates from the planned coordinates around the  $x$ -axis ( $\alpha$ , degrees),  $y$ -axis ( $\beta$ , degrees), and  $z$ -axis ( $\gamma$ , degrees) was calculated using the three markers [9,12]. Geometrical uncertainties were evaluated for both systematic and random external and internal errors [15]. The discrepancy of the actual coordinates of the center of gravity from the planned position in the manual set-up was regarded as the external error in the manual set-up. The external error in the gold marker set-up was the deviation of the center of gravity of the three gold markers from its planned position after the gold marker set-up. The intra-fractional motion of the marker during the irradiation was regarded as the internal error during the irradiation.

### 3. Results

Twelve patients (median age, 60 years; range, 33–78 years) with squamous cell carcinoma at the uterine cervix or stump of the cervix were enrolled after obtaining written consent for participating in the present study. Two patients experienced drop of a marker before CT scan and not treated with the 3DCB. The reason for the drop of the marker was not certain. There was no relationship between the size of the tumor and the drop of the marker. The discrepancy in distances between each marker at the first treatment day from the planning CT was distributed from 0 to 2.8 mm at the median of 0.8 mm in the 10 patients. These discrepancies were judged to be un-correctable and accepted to be used in the gold marker set-up. Thus, 83% (10 out of 12) eligible patients were treated with 3DCB as planned.

The 10 patients were available for the investigation of set-up error and internal organ motion. The external error in manual set-up was estimated from 48 measurements, the external error in gold marker set-up was estimated from 48 measurements, and the intra-fractional error was estimated from 105 measurements in the 10 patients.

The external error in manual set-up was  $0.4 \pm 3.6$ ,  $-0.6 \pm 4.5$ , and  $0.9 \pm 4.6$  mm (mean  $\pm$  SD) for the  $x$  (left-right),  $y$  (cranio-caudal), and  $z$  (antero-posterior) directions, respectively. The external error in gold marker set-up was  $1.0 \pm 1.2$ ,  $0.3 \pm 1.1$ , and  $0.9 \pm 1.7$  mm for the  $x$ ,  $y$ , and  $z$  directions, respectively. The 95% confidence interval of intra-fractional motion of the marker, or internal error during the irradiation, was 1.4–3.4, 1.9–2.5, and 2.4–4.2 mm in the  $x$ ,  $y$ , and  $z$  directions, respectively, for the treatment time of  $9.4 \pm 4.7$  min in the 10 patients. The table position required an average of 1.8 corrections (range: 0–6 corrections) in one treatment to correct the dislocation of the center of gravity more than 5 mm.

The standard deviation of the distribution of systematic deviations, total  $\Sigma(E+I)$  was 3.8, 4.6, and 4.9 mm in the  $x$ ,  $y$ , and  $z$  directions in the manual set-up using the  $\Sigma$  of external error and the  $\Sigma$  of internal error (Table 1). The total

Table 1  
Statistical analyses and estimated PTV-margin in manual set-up and marker set-up

		$x$ (mm)	$y$ (mm)	$z$ (mm)
$\Sigma(\text{ext})$	Manual	3.6	4.5	4.6
	Marker	2	2	2.1
$\Sigma(\text{int})$	Manual	1.2	1.1	1.7
	Marker	1.2	1.1	1.7
$\Sigma(\text{tot})$	Manual	3.8	4.6	4.9
	Marker	2.3	2.3	2.7
$\sigma(\text{tot})$	Manual	3.7	5.0	4.5
	Marker	3.3	3.0	4.2
$\sigma(\text{ext})$	Manual	2.8	4.7	3.1
	Marker	2.2	2.2	2.7
$\sigma(\text{int})$	Manual	2.4	2.1	3.2
	Marker	2.4	2.1	3.2
PTV-margin	Manual	10.2	12.8	12.9
	Marker	6.9	6.7	8.3

Sigma (ext): Sigma,  $\Sigma$ , for external error; Sigma (int): Sigma,  $\Sigma$ , for internal error; sigma (ext): sigma,  $\sigma$ , for external error; sigma (int): sigma,  $\sigma$ , for internal error. Sigma (tot): Sigma,  $\Sigma$ , for total error, taken as the systematic error; sigma (tot): sigma,  $\sigma$ , for total error, taken as the random error; PTV-margin:  $2\Sigma(\text{tot}) + 0.7\sigma(\text{tot})$ ; manual: manual set-up; marker: internal gold marker set-up.

$\Sigma(E+I)$  was reduced to 2.3, 2.3, and 2.7 mm in the set-up using the gold markers. The average standard deviation of the distribution of random deviations, total  $\sigma(E+I)$  was 3.7, 5.0, and 4.5 mm in the manual set-up using the  $\sigma$  of external error and the  $\sigma$  of internal error. The total  $\sigma(E+I)$  was 3.3, 3.0, and 4.2 mm in the gold marker set-up. The appropriate PTV margin was estimated to be 10.2, 12.8, and 12.9 mm in the manual set-up and 6.9, 6.7, and 8.3 mm in the gold marker set-up, respectively, using the equation PTV margin =  $2(\text{total } \Sigma) + 0.7(\text{total } \sigma)$  [13].

The mean rotational error was 0.5, 0.7, and  $-2.9^\circ$  for  $\alpha$ ,  $\beta$ , and  $\gamma$ , respectively. The standard deviation of systematic error of rotation was 7.6, 4.3, and  $3.8^\circ$  for  $\alpha$ ,  $\beta$ , and  $\gamma$ , respectively. The average random error of rotation was 8.4, 4.3, and  $3.0^\circ$  for  $\alpha$ ,  $\beta$ , and  $\gamma$ , respectively.

### 4. Discussion

Stroom et al. have shown that a PTV margin size which ensures at least 95% of the dose (on average) to 99% of the CTV of cervical cancer, appears to be about 1 cm (7 mm for systematic and random error of the pelvic bone and 3 mm for intra-pelvic organ motion and delineation error) [13]. The present study showed that the appropriate PTV margin was 10.2, 12.7, and 12.9 mm in the manual set-up for the  $x$ ,  $y$ , and  $z$  directions, and suggested that the estimation of Stroom et al. was reasonable. Stroom et al. have also shown that online set-up corrections using bony landmarks in anterior–posterior portal images during radiotherapy are useful to reduce the PTV margin reduction to about 5 mm [14]. However, Buchali et al. have examined the impact

of the filling status of the bladder on the movement of the uterus and concluded that the PTV margin should be 15 mm cranio-caudally [1]. Kaatee et al. recently investigated organ movement in patients with cervical cancer using fluoroscopic electronic portal imaging and radiopaque markers [4]. They reported that the internal cervical movement was considerably larger than the movement of the pelvic bony structures.

In the present study, the systematic and random external errors decreased significantly using the internal fiducial markers comparing to the manual set-up using skin markers. However, the PTV margin required in the gold marker set-up was larger than we had expected. The residual error in the gold marker set-up was probably due to the distortion of the soft tissue and/or internal organ motion during the period of set-up.

Since we did not use gated irradiation, there was no difference in internal error between the manual set-up and gold marker set-up in this protocol setting. The appropriate PTV margin was suggested to be 6.9, 6.7, and 8.3 mm for the lateral, cranio-caudal, and antero-posterior directions. Since we need to add margins for delineation error, deformation, and rotation error, the appropriate PTV margin must be 2–3 mm larger than these values.

There were several cases with the standard deviation of internal organ motion more than 5 mm. In fact, since the table position was corrected when the shift was more than 3–5 mm, there might have been more dislocation if the table position was not corrected during the irradiation. Thus, the appropriate PTV margins described above may be too small to use in the absence of frequent observations by orthogonal X-ray imaging during the irradiation.

In conclusion, set-up of gynecological malignancy using three markers and RTRT system was useful to reduce the uncertainty due to external and internal error but still requires at least 7–8 mm PTV margin. The fluoroscopic system and three gold markers would be a useful tool to realize individual-based, precise adaptive irradiation for the moving, shrinking, and deforming gynecological malignancy.

#### Acknowledgements

This study is partly supported by grant-in-aid for scientific research No. 16023207 from Japanese Ministry of Education, Culture, Sports, Science and Technology to Hokkaido University Hospital (H.S.).

#### References

- [1] Buchali A, Koswig S, Dinges S, et al. Impact of the filling status of the bladder and rectum on their integral dose distribution and the movement of the uterus in the treatment planning of gynaecological cancer. *Radiother Oncol* 1999;52:29–34.
- [2] Green JA, Kirwan JM, Tierney JF, et al. Survival and recurrence after concomitant chemotherapy and radiotherapy for cancer of the uterine cervix: a systematic review and meta-analysis. *Lancet* 2001;358:781–6.
- [3] Ito H, Shigematsu N, Kawada T, et al. Radiotherapy for centrally recurrent cervical cancer of the vaginal stump following hysterectomy. *Gynaecol Oncol* 1997;67:154–61.
- [4] Kaatee RS, Olofsen MJ, Verstraate MB, Quint S, Heijmen BJ. Detection of organ movement in cervix cancer patients using a fluoroscopic electronic portal imaging device and radiopaque markers. *Int J Radiat Oncol Biol Phys* 2002;54:576–83.
- [5] Kagei K, Shirato H, Nishioka T, et al. High-dose-rate intracavitary irradiation using linear source arrangement for stage II and III squamous cell carcinoma of the uterine cervix. *Radiother Oncol* 1998;47:207–13.
- [6] Kitamura K, Shirato H, Seppenwoolde Y, et al. Three-dimensional intra-fractional movement of prostate measured during real-time tumor-tracking radiotherapy in supine and prone treatment positions. *Int J Radiat Oncol Biol Phys* 2002;53:1117–23.
- [7] Kitamura K, Shirato H, Shimizu S, et al. Registration accuracy and possible migration of internal fiducial gold marker implanted in prostate and liver treated with real-time tumor-tracking radiation therapy (RTRT). *Radiother Oncol* 2002;62:275–81.
- [8] Nag S, Chao C, Erickson B, et al. The American Brachytherapy Society recommendations for low-dose-rate brachytherapy for carcinoma of the cervix. *Int J Radiat Oncol Biol Phys* 2002;52:33–48.
- [9] Onimaru R, Shirato H, Aoyama H, et al. Calculation of rotational setup error using the real-time tracking radiation therapy (RTRT) system and its application to the treatment of spinal Schwannoma. *Int J Radiat Oncol Biol Phys* 2002;54:939–47.
- [10] Shimizu S, Shirato H, Kitamura K, et al. Use of an implanted marker and real-time tracking of the marker for the positioning of prostate and bladder cancers. *Int J Radiat Oncol Biol Phys* 2000;48:1591–7.
- [11] Shirato H, Shimizu S, Kunieda T, et al. Physical aspects of a real-time tumor-tracking system for gated radiotherapy. *Int J Radiat Oncol Biol Phys* 2000;48:1187–95.
- [12] Shirato H, Harada T, Harabayashi T, et al. Feasibility of insertion/implantation of 2.0-mm-diameter gold internal fiducial markers for precise setup and real-time tumor tracking in radiotherapy. *Int J Radiat Oncol Biol Phys* 2003;56:240–7.
- [13] Stroom JC, de Boer HC, Huizenga H, Visser AG. Inclusion of geometrical uncertainties in radiotherapy treatment planning by means of coverage probability. *Int J Radiat Oncol Biol Phys* 1999;43:905–19.
- [14] Stroom JC, Olofsen-van Acht MJ, Quint S, et al. On-line set-up corrections during radiotherapy of patients with gynecologic tumors. *Int J Radiat Oncol Biol Phys* 2000;46:499–506.
- [15] Stroom JC, Heijmen BJ. Geometrical uncertainties, radiotherapy planning margins, and the ICRU-62 report. *Radiother Oncol* 2002;64:75–83.

《実際の治療方法》  
肺癌の放射線療法

早川和重

特集 肺 癌 — 内科医に必要な最新基礎知識

臨床雑誌「内 科」第95巻 第1号〔2005年1月号〕別 刷

南 江 堂

# 《実際の治療方法》 肺癌の放射線療法

早川和重\*

## 要 旨

- 非小細胞肺癌で根治的放射線療法の適応となるのは、臨床病期 Bulky N2 IIIA 期ならびに悪性胸水・胸膜播種・対側縦隔リンパ節転移を除く III B 期の局所進行癌と、I/II 期でも高齢などによる心・肺機能の低下や合併症のために医学的に切除不能と判断される症例である。
- 線量は通常分割照射法で 60 Gy/30 回以上が推奨される。
- 化学療法同時併用例では予防照射を省き GTV に限局して高線量を照射する傾向にある。
- 定位放射線照射や重粒子線治療など照射技術の進歩により、局所制御率・治療成績は向上しつつある。
- 正常組織の有害反応を抑えるため 3 次元治療計画を行い、DVH による被照射肺体積  $V_{20}$  を評価することが重要である。

## はじめに

肺癌の放射線治療には、① 切除不能非小細胞肺癌の根治的放射線治療、② 術前・術後照射、③ 小細胞肺癌の胸部照射、④ 小細胞肺癌の脳転移に対する予防的全脳照射、⑤ 広範囲な腫瘍進展や遠隔転移に伴う症状の緩和を目的とした対症的照射などがある<sup>1,2)</sup>。本稿では、①を中心に述べる。

## 非小細胞肺癌の放射線治療

### 1. 胸部照射の適応と治療方針

非小細胞肺癌で根治的放射線照射の適応となるのは、臨床病期 Bulky N2 IIIA 期および悪性胸水を除く III B 期の切除不能局所進行癌と、I・II 期でも高齢や合併症のために内科的に切除不能と判断される症例である (Table 1)<sup>1,3)</sup>。さらに、局所進行癌では、高齢者や PS 不良例を除けば化学療法と

の併用が原則となる (他稿)。

### 2. 分割照射法と線量

通常の放射線治療では、1 日 1 回 1.8~2 Gy で週 5 日照射する単純分割照射 (CF) 法が用いられている (Fig. 1)<sup>3,4)</sup>。これは、正常組織と腫瘍組織とのあいだで放射線感受性や照射後の回復に差がみられることを利用して確立された照射法である。CF 法で腫瘍制御に要する線量として、顕微鏡的な腫瘍細胞量に対しては 40~50 Gy、肉眼的腫瘍には 60 Gy 30 回 (6 週) 以上の線量が必要となる。

分割照射法の工夫としては、1 日 2 回以上照射を行う多分割照射 (MFD) 法と 1 回線量を多くして照射回数を少なくする少分割照射法 (hypofractionation) がある (Fig. 1)<sup>3,4)</sup>。MFD 法の照射間隔は、正常組織が照射後の亜致死障害から回復する 4 時間以上とするのが原則で、遅発性有害反応を抑えるためには 6 時間以上空けるほうがよい。そのため、日常臨床では時間的制約から 1 日 2 回が

\* K. Hayakawa (教授)：北里大学放射線科学。

Table 1. 非小細胞肺癌の放射線治療に関する病期別治療指針案

臨床病期分類		実地医療	探索的医療(臨床試験)
I 期		外科切除 放射線療法(内科的切除不能)	切除+術後補助療法(T2) 定位放射線照射(T1)
II 期		外科切除 放射線療法(内科的切除不能) 術前照射±治療+切除	周術期補助療法+切除 化学放射線療法
T3N0(superior sulcus を含む胸壁浸潤型)			
III A 期			
T3N1		外科切除	周術期補助療法+切除
T1~3N2(手術ではじめて N2 が判明した病理学的 N2 は除く)			
N2 節外浸潤(-)	単一ステーション 複数ステーション	外科切除 周術期補助療法+切除 化学放射線療法*	周術期補助療法+切除 周術期補助療法+切除 化学放射線療法
節外浸潤(+)		化学放射線療法*	放射線療法+新規抗癌薬
Bulky N2(単純 X 線写真, 気管支鏡で所見あり)		化学放射線療法*	化学放射線療法+分子標的薬剤
III B 期			
T4N0~1	同一肺葉内転移 左房浸潤, 気管分岐部浸潤*, superior sulcus tumor の一部	外科切除 外科切除 (含, 再建術 <sup>†</sup> )	周術期補助療法+切除 周術期補助療法+切除
T1~4N3	悪性胸膜炎 その他	化学放射線療法* 对症療法(胸膜癒着術) 化学放射線療法*	新規抗癌薬, 分子標的薬剤 周術期補助療法+切除 放射線療法+新規抗癌薬 化学放射線療法+分子標的薬剤

†: sleeve pneumonectomy, \*: 高齢者・PS 不良例は除く。

[文献 1, 3)より引用, 改変]

一般的である。さらに MFD 法には過分割照射(HF)法(1.1~1.2 Gy/回), 加速分割照射(AF)法(1.8~2 Gy/回), 加速過分割照射(AHF)法(1.5 Gy/回)がある。HF 法は遅発性有害反応の増強を抑えて総線量を増加する方法で, 局所進行癌に対する 1.2 Gy/回法では 69.6 Gy が至適線量として推奨されている<sup>5)</sup>。AF, AHF 法は, 生残腫瘍細胞の再増殖が照射開始後約 4 週以降に加速することから照射期間の短縮を目的とした照射法である。AF は午後の照射野を肉眼的腫瘍体積(gross tumor volume: GTV)に局限した field within a field (concomitant boost) 照射<sup>6)</sup>として行われることが多い。AHF 法では, 1.5 Gy/回で 1 日 3 回 12 日間 54 Gy 照射する連続加速過分割放射線治療(CHART)法<sup>9)</sup>の有用性が示されている。MFD 法は CF 法に比べて急性期の有害反応が増強するた

め, その軽減対策が課題である。

少分割照射法は一般的には姑息・対症的照射法として用いられているが, 根治照射として 1 回線量 2.5~2.75 Gy で総線量 60~66 Gy 照射する方法<sup>7)</sup>もある。また, 定位照射では照射野が小さいため短期照射が可能で, 1 回 10~15 Gy での 40~60 Gy の照射が行われている<sup>8)</sup>。

CF 法や MFD 法で治療期間中に 2 週程度の休止期間を置く split course 照射法は, 治療中に腫瘍の再増殖が起こるため望ましくないとされているが<sup>5)</sup>, 高齢者の入院期間短縮への対応策として行われることもある。

放射線治療では線量に応じて確率的に腫瘍細胞量が減少していくために, 放射線治療による腫瘍制御の可能性は腫瘍細胞量に依存する。また, 腫瘍サイズが大きくなると放射線感受性の低い低酸

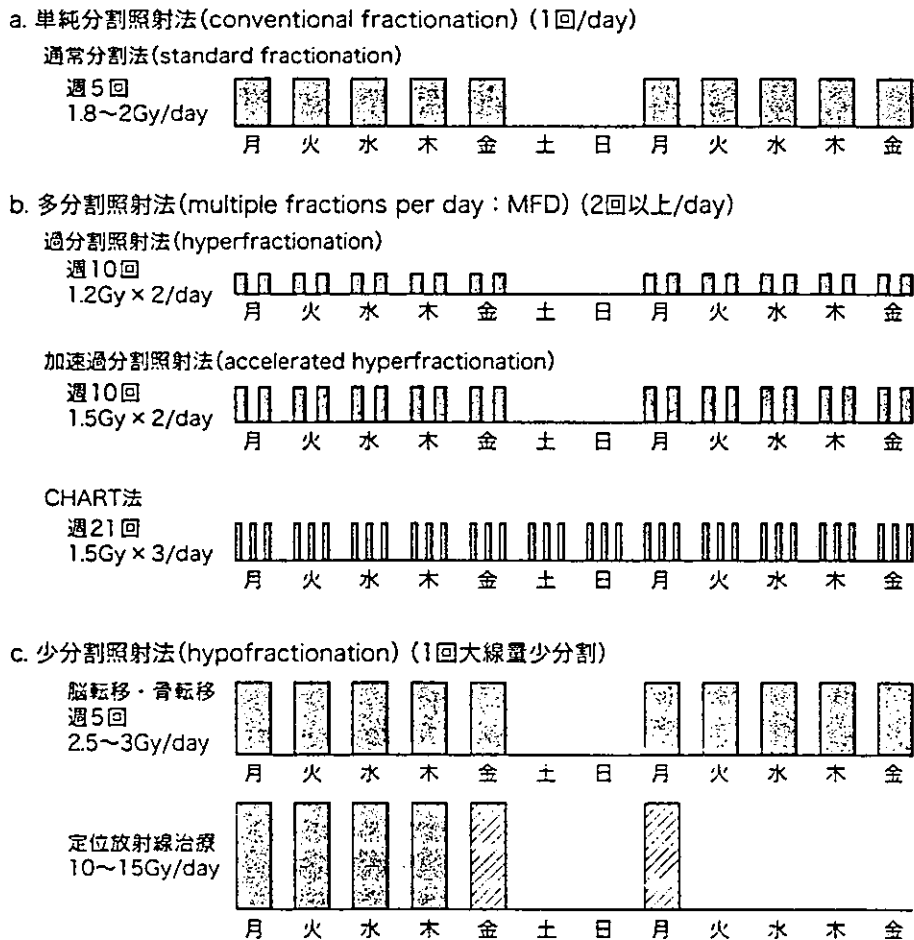


Fig. 1. 肺癌に用いられている分割照射法

CHART法はわが国の実地医療では現実的ではないが、照射野の工夫で1日3回照射は可能である。  
 [文献3)より引用、改変]

素細胞の割合も高くなる。したがって、腫瘍サイズが大きいくほど大線量が必要となる<sup>1~4)</sup>。Jeremicら<sup>9)</sup>は、I・II期例について種々の線量分割照射法を含めた線量-効果関係のレビューを行い、根治線量としてCF法での65~70 Gy相当以上の線量が推奨されるとしている。ただし、肺門部への80 Gy以上の照射は耐容線量を超えていると考えられる<sup>1~4)</sup>。

### 3. 照射野

局所進行癌の照射野は原発巣、同側肺門、縦隔を含めるのが標準的である (Fig. 2)<sup>1~4)</sup>。照射野辺縁は呼吸性移動などを考慮し、腫瘍辺縁から1.5~2 cm、予防的照射範囲 (臨床標的体積 (CTV))

では1 cm前後とする。なお、有害事象として grade 2以上の放射線肺臓炎の発症を抑えるためには、20 Gy以上照射される正常肺の体積  $V_{20}$ が、放射線単独の場合には正常肺全体の体積の40%を超えないよう (できるだけ35%以下になるよう)<sup>1~3)</sup>に、化学療法併用例では25%を超えないように計画する<sup>3)</sup>。線量体積ヒストグラム (dose volume histogram : DVH)で評価できない場合には、目安としてX線シミュレータ写真上で照射野が片側肺の1/2 (右上葉または左上区原発の場合には2/3)を超えないようにする。原発巣が肺末梢部にある症例では、照射野の縮小時に原発巣と転移リンパ節に照射野を分けて照射する方法も考慮す

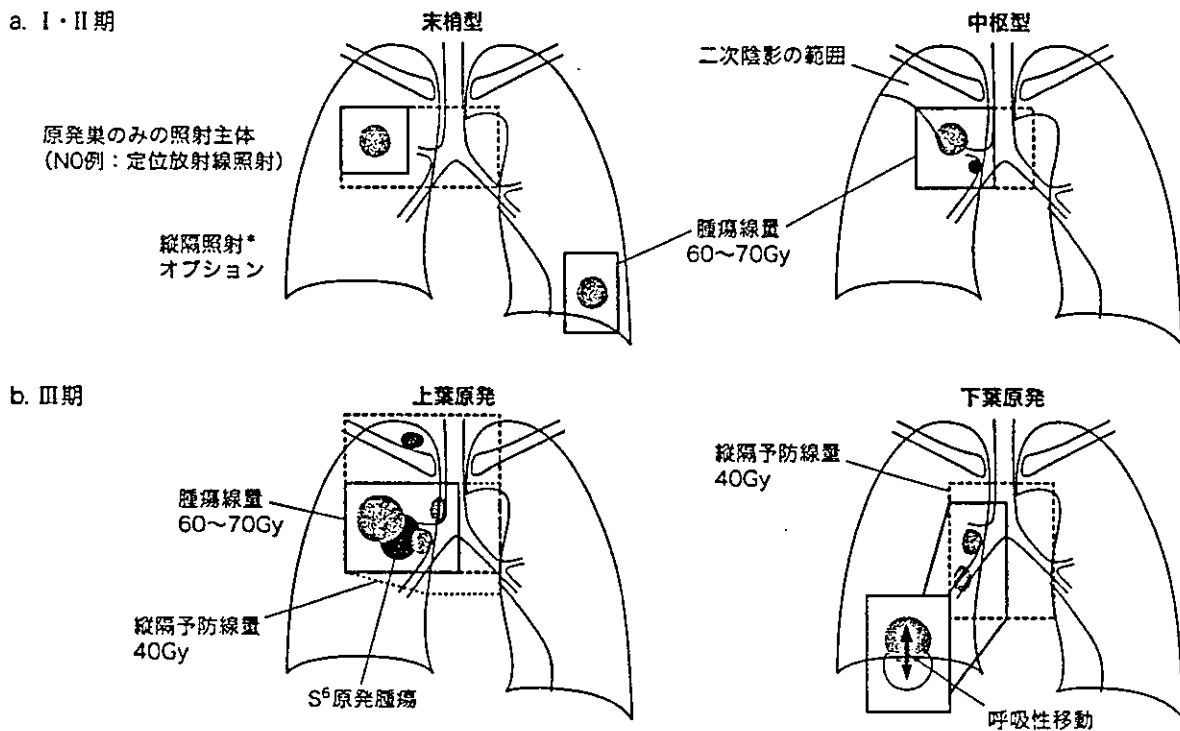


Fig. 2. 非小細胞肺癌の根治的放射線治療の照射野

- a : 末梢型 NO 例は低肺機能例が対象となることが多く、予防的縦隔照射は必ずしも行わなくてよい。中枢型はリンパ節転移のリスクも高く、所属リンパ節を含めても照射野が大きくならないので、肺門・縦隔への予防照射を行う(\*とくに扁平上皮癌)。
- b : 上葉あるいは下葉 S<sup>6</sup> 原発例では、他部位の原発例と比べて比較的小きな照射野で縦隔の転移リンパ節を含めることができる。また、上葉原発例では、同側鎖骨上窩リンパ節まで照射野に含めても照射野は大きくならない。一方、下葉原発例では、腫瘍の呼吸性移動により、さらに照射野は大きくなる。

[文献 1~4) より引用, 改変]

べきである。高齢者や低肺機能患者では可能な限り縦隔・肺門への照射は避けるほうが望ましい。とくに、末梢発生 I 期例では、原発巣に局限した照射でも縦隔リンパ節のみの再発は少ない<sup>10)</sup>。

通常の縦隔を含む照射野では前後対向 2 門で、40~45 Gy まで照射し、その後、脊髄を外して斜入対向 2 門照射に変更されることが多い。ただし、最初の治療計画で脊髄の 1 回最大線量が 2 Gy を超えないように注意する。また、変更時、腫瘍の縮小に応じて GTV に局限して照射野を縮小するのが一般的である。

#### 4. 所属リンパ節予防照射

リンパ節転移の特徴を組織型別にみると、扁平上皮癌は肺門・縦隔へと順次性に転移していくが、腺癌では非順次性に進展する傾向が認められ

る<sup>2)</sup>。また、腺癌の縦隔リンパ節転移例では遠隔転移頻度も高く、所属リンパ節への予防照射は扁平上皮癌で意義が大きいと考えられる。上縦隔、鎖骨上窩リンパ節転移例では鎖骨上窩も照射野に含めるが、上葉あるいは S<sup>6</sup> 原発例では肺門・縦隔さらに鎖骨上窩までを一緒に照射しても照射野が比較的小さくできるので有利である (Fig. 2)。両側肺門部を含む照射は肺機能に大きな影響を及ぼすばかりでなく、重篤な肺臓炎のリスクも高くなるので避けるべきである。

局所進行癌に対する同時化学療法併用例では、微視的転移巣は化学療法に期待し、有害反応の軽減を目的に GTV に局限した照射野を設定し、3 次的に線量を増加する方法が主流になりつつある。



Table 2. I期非小細胞肺癌に対する定位放射線照射の治療成績

報告者	症例数	照射線量 (Gy)	1回線量 (Gy)	他病死 (%)	局所制御率 (%)	生存率 (%)	原病生存率 (%)
Uematsu	50	50~60	(5~)10	22	94	66(3年)	88(3年)
Nagata	16(IA期)	48	12	6	100	79(2年)	NA
Takai	17	45~60	7.5~15	12	82	73(4年)	84(4年)

NA: not available

[文献12)より引用]

### 5. 定位放射線照射

末梢小型I期非小細胞肺癌に対しては定位放射線照射が検討されている。Uematsuらの報告<sup>11)</sup>では、原発巣のみへの定位放射線治療で3年生存率66%、3年原病生存率88%と良好な治療成績が示されている。Nagataら<sup>8)</sup>も16例のT1肺癌に対して中心線量48Gy/4回の定位照射を行い、観察期間6~36ヵ月(中央値19ヵ月)で、すべて局所制御されていると報告している(Table 2)<sup>12)</sup>。定位照射による腫瘍制御率の向上には大きな期待が寄せられているが、至適分割照射法については今後の重要な検討課題である。

### 陽子線・重粒子線治療の現状○

陽子線や重イオン線を用いた照射は放射線の飛程が一定の深さまでにとどまる性格を有しており、数方向から照射すれば正常組織の損傷を軽微にとどめながら十分な腫瘍制御線量の照射が可能で、3次元照射に適している。放射線医学総合研究所で行われている炭素線治療は、殺細胞効果に優れており、末梢型非小細胞肺癌に対するI/II相試験では良好な治療結果が得られている<sup>13)</sup>。それによると、腫瘍の大きさがT2でも通常の光子に換算して86.4Gy/18回あるいは72Gy/9回以上の照射を行えば90~95%局所制御可能であり、正常肺組織への影響も軽微であることがわかってきた。これらのデータは今後の陽子線治療や3次元原体照射・定位照射の発展に大いに寄与することが期待されている。

### 化学療法併用時の留意点<sup>2)</sup>○

化学療法を併用しても通常分割照射法での必要な推奨線量は最低60Gy/6~7週である<sup>14)</sup>。また、同時併用では、急性障害の軽減のためにスプリットコース照射法としても、照射休止期間の生存に対する不利益は明らかではない<sup>1~3)</sup>。

放射線併用時の薬剤の安全性については、放射線との相性が重要で、cisplatinあるいはetoposideは放射線と比較的安全に併用できる薬剤である。irinotecanとの同時併用では、肺臓炎や食道炎などの非血液毒性のリスクが高く検討が必要である<sup>5)</sup>。なお、わが国ではgemcitabineと放射線との同時併用は禁忌である。

### 胸部照射の副作用対策○

局所進行肺癌に対する放射線治療でもっとも注意を払うのが脊髄に対する影響である。通常分割照射法の場合、40Gy程度では脊髄症が発症することはないが、50Gy以上の線量は耐容線量を超えていると考えられている<sup>1~4)</sup>。また、脊髄のような遅発性反応が問題となる臓器は1回線量が大きくなると耐容線量が低下する。したがって、治療の際に脊髄の1回最大線量が2Gyを超えないように配慮する必要がある。最近では1回1.2Gy程度の多分割照射法が慢性障害を軽減させる方法として期待されているが、照射間隔は6時間以上空けたほうがよい。

放射線肺臓炎は通常は照射野に一致してみられるもので、肺癌治療線量以下の50Gyで必発である。したがって、被照射肺の範囲を小さくする配

慮が肝要である。先に述べた 20 Gy 以上照射される正常肺の体積  $V_{20}$  に配慮した治療計画を行うことが推奨される。とくに化学療法との同時併用例では、 $V_{10}$  および  $V_{20}$  が大きくなると重篤な肺臓炎発症のリスクが高くなるため<sup>1-3)</sup>、照射野の設定は慎重に行う必要がある。


放射線食道炎は多分割照射や化学療法の併用時に治療を中断せざるをえないほど高度となることもあるが、通常分割法による照射単独療法ではほとんど問題とはならない。心臓は 40 Gy 以上照射されると組織学的な変化は認められるようになるが、部分的照射であれば 60 Gy 以上の照射でも臨床的に問題となることはまれである。化学療法が併用された場合には注意を要する。

#### 文 献

- 1) 早川和重：I-Ⅲ期非細胞癌の治療：肺癌診療ガイドラインに基づくコンセンサスと新たな臨床試験の動向：手術適応外症例の治療方針：放射線療法。日胸 63：741, 2004
- 2) 早川和重：肺癌に対する放射線治療。日本医会誌 63：533, 2003
- 3) 早川和重、北野雅史：肺がんに対する放射線治療の原則。癌の臨 49：1265, 2003
- 4) 早川和重：胸部照射、脳照射。肺癌：患者へのアプローチから治療の最前線まで、福岡正博、西條長宏(編)、第2版、南江堂、東京、p96-104, 2003
- 5) 有吉 寛ほか：肺癌の放射線治療。EBMの手法による

る肺癌診療ガイドライン、EBMの手法による肺癌の診療ガイドライン策定に関する研究班(主任：藤村重文)(編)、金原出版、東京、p39-70, 2003

- 6) Saunders MI: Programming of radiotherapy in the treatment of non-small-cell lung cancer: a way to advance care. Lancet Oncol 2: 401, 2001
- 7) Baumann M et al: Dose and fractionation concepts in the primary radiotherapy of non-small cell lung cancer. Lung Cancer 33[Suppl 1]: S35, 2001
- 8) 永田 靖ほか：高精度放射線治療。日獨医報 49: 286, 2004
- 9) Jeremic B et al: Radiotherapy alone in technically operable, medically inoperable, early-stage (I/II) non-small-cell lung cancer. Int J Radiat Oncol Biol Phys 54: 119, 2002
- 10) Rowell NP, Williams CJ: Radical radiotherapy for stage I/II non-small cell lung cancer in patients not sufficiently fit for or declining surgery (medically inoperable): a systematic review. Thorax 56: 628, 2001
- 11) Uematsu M et al: Computed tomography-guided frameless stereotactic radiotherapy for stage I non-small cell lung cancer: a 5-year experience. Int J Radiat Oncol Biol Phys 51: 666, 2001
- 12) 早川和重：非小細胞肺癌：放射線療法。MOOK 肺癌の臨床 Annual Review 2003。加藤治文ほか(監)、篠原出版新社、東京、p195-203, 2003
- 13) Miyamoto T et al: Carbon ion radiotherapy for stage I non-small cell lung cancer. Radiother Oncol 66: 127, 2003
- 14) Pfister DG et al: American Society of Clinical Oncology treatment of unresectable non-small-cell lung cancer guideline: update 2003. J Clin Oncol 22: 330, 2004



**皮膚疾患  
最新の治療  
2003-2004**

**発売中**

## 皮膚疾患最新の治療2003-2004

●編集 新村真人 東京慈恵会医科大学教授・瀧川雅浩 浜松医科大学教授

2年ごとの刊行で、皮膚疾患治療の最新情報を提供。疾患ごとに、治療方針、処方例、生活指導を具体的に示し日常診療の指針として役立つ。さらに最近の知見をトピックスとして盛り込む。巻頭特集は「アトピー性皮膚炎の治療」と「ケミカルピーリング」。巻末には詳細な薬剤一覧を収載。皮膚疾患の診療にかかわるすべての医師、ナース、薬剤師に必携の実用書。

■B5判/270頁 定価8,400円(本体8,000円+税5%) 2003.1.第1版

# 南江堂

綜合臨牀 第54卷 第1号  
(平成17年1月1日発行 別冊)

## 前立腺癌に対する新しい放射線治療

*Current radiation therapy for prostate cancer*

佐藤 威文  
SATOH Takefumi

陳 偉強  
CHEN Weigiang

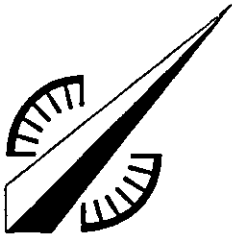
北野 雅史  
KITANO Masashi

早川 和重  
HAYAKAWA Kazushige

石山 博條  
ISHIYAMA Hironichi

馬場 志郎  
BABA Shiro

永 井 書 店



診断の指針  
治療の指針

## 前立腺癌に対する新しい放射線治療

Current radiation therapy for prostate cancer

佐藤 威文\*<sup>2</sup> 北野 雅史\*<sup>4</sup> 石山 博條\*<sup>4</sup>  
 SATOH Takefumi KITANO Masashi ISHIYAMA Hiromichi  
 陳 偉強\*<sup>1</sup> 早川 和重\*<sup>5</sup> 馬場 志郎\*<sup>3</sup>  
 CHEN Weigiang HAYAKAWA Kazushige BABA Shiro

はじめに

血清前立腺特異抗原(PSA)測定が臨床導入された1986年来、前立腺癌検出効率は飛躍的に向上し、欧米のみならず本邦においても、その発症頻度は急激に増加してきている。1994年における本邦での罹患数は10,940人であったが、2015年には30,285人へと著しい増加が予測されている。また米国においても、2003年度は200,900人が新たに前立腺癌と診断され、成人男性における最も罹患率の高い癌として大きな社会問題となっている。このような背景の中、より早期で病気が発見される“Early detection”は日米共通の傾向であり、根治的前立腺全摘除術が施行された全体の60%がorgan confinedであった結果も確認されている。しかし一方で、より侵襲の少ない“Less invasive”を望む社会的な潮流も加わり、このようなlow risk群を含めた増加に伴う密封小線源療法等の適応・希望症例の急激な増加が予測されている。

また近年の放射線治療機器の進歩や、コンピュータソフトの開発・導入により、その放射線治療技術も格段に向上し、外照射においても前立腺にのみ照射を集約・制御できることが可能になってきており、その治療法も多岐にわたってきている。

このような背景の中、本稿においては前立腺癌に対する新しい放射線治療として、北里大学病院で現在施行されている2種の密封小線源療法(<sup>125</sup>I low-dose rate brachytherapy: 図1, <sup>192</sup>Ir high-dose rate brachytherapy: 図2), ならびに新しい外照射法である3次元原体照射法(3D-CRT), および強度変調放射線治療(IMRT)について言及する。

### 1. 密封小線源療法: 永久刺入組織内照射(<sup>125</sup>I, LDR: low-dose rate brachytherapy)

同治療法については、すでに先行する米国において10年を超える治療歴があるも、本邦においてはその取り扱いにおける法的な整備がこれまで定められておら

ず、平成15年3月に「診療用放射線器具を永久的に挿入された患者の退出基準」が正式に厚生労働省から通達され、国内においても治療が開始された経緯がある。同治療は、<sup>125</sup>I(半減期59.4日)や<sup>103</sup>Pd(半減期17.0日)等の低線量率放射線物質を経会陰的に挿入し、前立腺内部から持続的に照射を行い、根治を狙う治療法である。その治療適応については、いわゆる予後の良いとされるlow risk群が適しているとされており、米国密封小線源療法学会(ABS: American Brachytherapy Society)の推奨は、臨床病期T1-T2a, かつGleason score 6以下, かつPSA 10ng/ml未満を同治療の単独療法の適応としており、いわゆるhigh risk groupとされる臨床病期T2b-c, またはGleason Score 8-10, またはPSA 20ng/ml以上の症例については、boostとしての外照射の併用を推奨している。また、この治療における厳格な年齢上限や前立腺体積等は定められていないものの、同じくABSでは5年以上の余命が期待され、前立腺体積が60cc未満の症例を主な適応条件としており、これを上回る前立腺体積を有する症

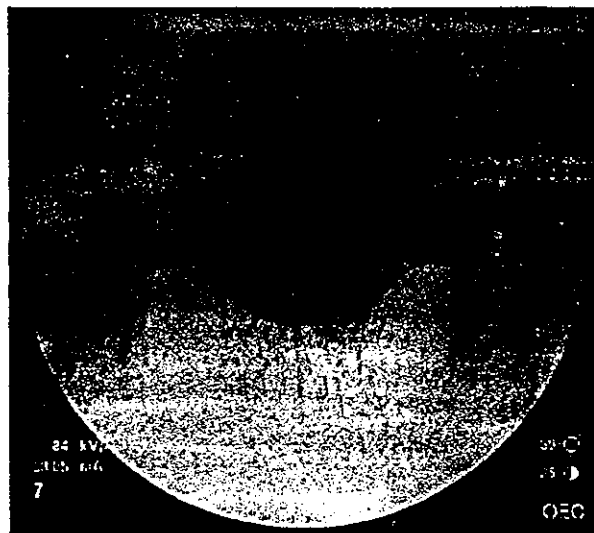


図1 LDR brachytherapy

\*北里大学医学部泌尿器科学 \*診療講師 \*教授 \*同 放射線科学 \*教授  
 Key words 前立腺癌 放射線治療 密封小線源療法